



How to mitigate flood events similar to the 1979 catastrophic floods in lower Tagus

Diego Fernández-Nóvoa^{1,2}, Alexandre M. Ramos², José González-Cao¹, Orlando García-Feal¹, Cristina
5 Catita², Moncho Gómez-Gesteira¹, Ricardo M. Trigo^{2,3}

¹Centro de Investigación Mariña (CIM), Universidade de Vigo, Environmental Physics Laboratory (EPhysLab), Campus da
Auga, 32004 Ourense, Spain

²Instituto Dom Luiz (IDL), Faculdade de Ciências da Universidade de Lisboa, 1749-016 Lisbon, Portugal

10 ³Departamento de Meteorologia, Universidade Federal Do Rio de Janeiro, Rio de Janeiro, Brazil

Correspondence to: Diego Fernández-Nóvoa (diefernandez@uvigo.es)

15

Abstract. The floods that struck lower Tagus valley in February 1979 correspond to the most intense floods in this river and affected the largest number of people in a river flow event in Portugal, during the last 150 years. In fact, the vast area affected impacted significantly circa 10k people in the lower Tagus sector (and an additional 7k in other regions of Portugal), including thousands of people evacuated or made homeless. In this context, the present study focuses on an in depth analysis
20 of this event from a hydrodynamic perspective by means of Iber+ numerical model and on developing strategies to mitigate the flood episodes that occur in the lower section of the Tagus river using the outstanding floods of February 1979 as benchmark. In this sense, several large dams and reservoirs are located along the Tagus river basin, and for that, dam operating strategies were developed and analyzed to take advantage of these infrastructures to minimize the effect of floods. Overall, the numerical results indicate a good agreement with water marks and some descriptions of the 1979 flood event,
25 which demonstrates the model capability to evaluate floods in the area under study. Regarding flood mitigation, obtained results indicate that the frequency of floods can be reduced with the proposed strategies. In addition, hydraulic simulations corroborated an important decrease in water depth and velocity for the most extreme flood events, and also a certain reduction of flood extension was detected. This confirms the effectiveness of the proposed strategies to help in reducing flood impact in lower Tagus valley through the efficient functioning of dams.

30



1 Introduction

Iberian Peninsula corresponds to a relevant region that has been historically affected by important river floods (Benito et al., 1996; 2003; Pereira et al., 2016; Rebelo et al., 2018; Santos et al., 2018; González-Cao et al., 2021; 2022). In particular, its western area is especially vulnerable to these phenomena since it can be directly affected by the storm-tracks of the Northern Hemisphere that transport heat and moisture (Peixoto and Oort, 1992; Trigo, 2006). Some specific synoptic features can favor extreme weather conditions that promote high precipitation rates and thus important associated river floods (Trigo and DaCamara, 2000; Trigo, 2006; Rebelo et al., 2018). In this context, in the last decade there has been a steep increment of works dealing with historical river floods that took place in the western half of the Iberian Peninsula, namely the floods that occurred in the Minho, Lima and Douro basins in 1909 (Pereira et al., 2016), in the Tagus basin in 1876 and 1979 (Benito et al., 2003; Salgueiro et al., 2013; Trigo et al., 2014; Rebelo et al., 2018), or in the Guadiana basin in 1876 (Trigo et al., 2014; González-Cao et al., 2021). The floods that struck lower Tagus valley from February 5 to 16, 1979 correspond to the most intense occurred in this river since, at least, the mid-19th century. Additionally, this outstanding event also implied to the largest number of people affected in the Iberian Peninsula in a river flood event in the last 150 years. The area affected by prolonged precipitation is much larger, thus other regions of western Iberia were also seriously affected. In fact, the vast area affected impacted roughly 10k people in the lower Tagus sector (and an additional 7k in other regions of Portugal), including thousands of people evacuated or made homeless. A detailed description of the causes behind this event and its main consequences can be found in Rebelo et al. (2018). Unlike previous more historical events (such as the 1876 floods), in 1979 there were already several large dams and reservoirs in both the Spanish and Portuguese sections of the Tagus river basin. These structures could have mitigated the amplitude of the flood, since dams are one of the main mechanisms that can play an important role in flood reduction (Lee et al., 2009; Valeriano et al., 2010; Chou and Wu, 2015). However, lack of communications between the management authorities in both countries at the time was translated in poor dam operations, leading to bad performance in terms of mitigating the 1979 flood (Rebelo et al., 2018). Thus, the main aims of the present study are to reproduce and analyze this historical event from a hydrologic-hydraulic point of view using the Iber+ numerical model, as well as developing dam operating strategies to mitigate the flood episodes that occur in the lower section of the Tagus river using the outstanding floods of February 1979 as benchmark. The effectiveness of the strategies proposed in terms of reducing the flood impact will be evaluated by means of numerical model simulations. This will contribute to address the flood mitigation challenges that the scientific community will face in the coming decades (IPCC, 2012; 2021), also taking into account that the increasing temperatures due to the significant rates of global warming contribute to the recent and future increase of extreme precipitation and floods in some parts of the world (Dankers and Feyen, 2008; Petrow and Merz, 2009; Alfieri et al., 2015; 2017; Diakakis, 2016; Arnell and Gosling, 2016; Modarres et al., 2016; ; Jongman, 2018; IPCC 2021), including vast areas of the Iberian Peninsula (Lorenzo and Alvarez, 2020). Additionally, this study also intends to prove that with open data and free applications for modeling, the results are satisfactory enough to apply the methodology proposed here in other regions where more detailed data may be scarce or non-existent.



This document is organized as follows: in Section 2 a brief description of the area under scope is presented. In Section 3, the data required to develop the study and the hydrodynamic model used are briefly described. Section 4 is devoted to results, including: i) testing different Digital Elevation Models (DEM) to select the most accurate for the area under scope, ii) the modelling and in-depth analysis of the flood registered in 1979 in lower Tagus valley, iii) a proposal of dam operating strategies to mitigate lower Tagus floods, including the analysis of their effectiveness taking advantage of the flood information provided by the hydraulic model. Finally, the main conclusions are summarized in section 5.

70

2 Area of study

The international Tagus basin is the largest river basin located in the Iberian Peninsula, draining more than 80,000 km² (approximately 70% in Spain and 30% in Portugal) (Ramos and Reis, 2001). The Tagus river flows from an elevation close to 1600 m.a.s.l. in the headwaters (Sierra de Albarracín, Spain) to sea level at its mouth in the Atlantic Ocean in Lisbon, with an approximate length of 1100 km (Agência Portuguesa do Ambiente, 2016) (Figure 1). Its flow is characterized by a pluvial regime with higher discharges in winter months and lower ones in summer, with a mean discharge of approximately 450 m³s⁻¹ (Ramos and Reis, 2001; Fernández-Nóvoa et al., 2017). The natural regime of the Tagus river was highly modified following the construction of several reservoirs in the main river but also in some of its tributaries. Among them, the Alcántara dam stands out by its sheer volume, located on the border between Spain and Portugal (Figure 1), with a total capacity surpassing 3160 hm³, being the second most important reservoir in the Iberian Peninsula and presenting a high capacity for flow retention. It drains a total extent larger than 50,000 km², which supposes about 70% of the total extent of Tagus basin.

Finally, it is important to remark that the particular characteristics of the lower Tagus valley are especially relevant for the scope of this study. This valley is characterized by a Cenozoic sedimentary basin, with a large and flattened alluvial plain, which promotes that floods can affect large extensions causing important damages (Rebelo et al., 2018) (Figure 1). This makes this area highly susceptible to periodic flooding associated with different phenomena, such as upstream hydrological flood, downstream tidal floods or storm surge (Vargas et al., 2008; Rocha et al., 2020; Lopes et al., 2022).



3 Data and Methods

90 3.1 Precipitation data

Precipitation data for the area under scope were obtained from Iberia01 database (Herrera et al., 2019). This dataset provides daily precipitation data with the highest spatial resolution of 0.1° covering the entire Iberian Peninsula available at the moment. It was produced using a dense network of stations spanning the period 1971-2015. Data are freely available on <https://doi.org/10.20350/digitalCSIC/8641>.

95 3.2 River discharge data

Daily mean Tagus river discharge data at the Almourol station (Figure 1) were downloaded from the SNIRH (Sistema Nacional de Informação de Recursos Hídricos) database for the period 1973-2021. The SNIRH is the National Information System on Water Resources of Portugal, whose data are freely available on www.snirh.pt.

3.3 Water level marks

100 Information of the level reached by the water in different points of the lower Tagus valley during the flood event that occurred in February 1979, were also obtained from the SNIRH database (see control points (black circles) in Figure 1).

3.4 Alcántara Dam data

Daily outflow and volume data at the Alcántara dam were provided by CEDEX (Centro de Estudios y Experimentación de Obras Públicas) for the period 1970-2018. CEDEX is the Spanish institution in charge of managing part of the hydrologic
105 data of the country, which are freely available on <http://www.cedex.es/>.

3.5 Hydraulic model

Iber is a numerical model that solves the 2D depth-averaged shallow water equations applying the finite volume methodology (Bladé et al., 2014). Recently, this code was improved by means of a new implementation in C++ and CUDA, resulting in the Iber+ (García-Feal et al., 2018). This improved model allowed for a much higher efficiency of the
110 simulations achieving a speed-up of two-orders of magnitude while maintaining the same precision. This was possible by using GPU (graphical processing unit) computing and HPC (high performance computing) techniques. This reduction in computation times allows dealing with large spatial domains and long-term events, thus providing a high capacity to simulate flood events with high accuracy (García-Feal et al., 2018; Fernández-Nóvoa et al., 2020; Bermúdez et al., 2021; Bonasia and Ceragene, 2021; González-Cao et al., 2021). Iber+ software is freely available for download from its official
115 website (<https://iberaula.es>).



In the present study, Iber+ was used to study flood events in the lower Tagus valley and to analyze the effectiveness of several dam operating strategies in terms of flood mitigation. For that, the domain defined in Iber+ includes the Tagus basin from Almourol to its mouth in Mar da Palha (the large basin in the estuary of the Tagus River near its mouth) at Lisbon (Figure 1). The inlet is defined as a Critical/Subcritical condition by adding the daily mean river flow registered in Almourol station, whereas the outlet of the domain is defined by means of a Supercritical/Critical condition. Precipitation data from Iberia01 were included in the domain being the infiltration computed by means of SCS-CN methodology (Mockus, 1964) and according to data provided by GCN250 (Jaafar et al., 2019). The spatial patterns of different land uses were defined using CORINE land cover data (CLC, 2000).

The entire domain was discretized using a mesh of unstructured triangles with sizes varying from 25m to 100m and surpassing 6M elements.

Several simulations were used here. The first (*Simulation_Control_1979*) merely tries to reproduce the observed spatial extension and depth of the flood observed in the lower Tagus section in the 1979 event, considering the historical timing and magnitude of water released by the main dams upstream as well as the precipitation downstream. The remaining simulations (*Simulation_Dam*), deal with artificial changes imposed on the dams with the aim of mitigating the flood magnitude in the lower Tagus area.

3.6 Digital Elevation Models (DEMs)

Different widely used and tested freely available global DEMs (Mukherjee et al., 2013; Szabó, 2015; Becek et al., 2016; Carrera-Hernandez, 2021; Guth and Geoffroy, 2021) were evaluated to select the most suitable one to reproduce the floods in the area under scope. The analyzed DEMs were: i) ESRI-DEM for Portugal mainland was made available by ESRI Portugal (ESRI copyright ©) through the ArcGIS online platform (downloadable from www.arcgis.com/home/search.html?t=content&q=owner:ESRI-PT). This DEM is based on data obtained by the Terra-ASTER (Advanced Spaceborn Thermal Emission and Reflection Radiometer) sensor adapted to Portugal; ii) ASTER-GDEM obtained by photogrammetric methods from the Japanese ASTER-VNIR sensor (infra-red nadir and backwards sensors with 15 m GSD) and provided by NASA Earth Data and from Japan Space Systems (downloadable from the USGS <https://earthexplorer.usgs.gov/>); iii) SRTM-DEM obtained by the Shuttle Radar Topography Mission by SAR Interferometry (downloadable from the USGS, <https://earthexplorer.usgs.gov/>); iv) Copernicus DEM (COP-DEM GLO-30) provided by the European Space Agency (ESA) and AIRBUS. This DEM is based on the WorldDEM™, which is in turn based on edited and smoothed radar satellite data acquired during the TanDEM-X mission (downloadable from ESA's Copernicus Space Component Data Access (CSCDA) system, <https://panda.copernicus.eu/>). Some original characteristics of these DEMs are specified in Table S1 of Supplementary Material. All the databases are freely available and provide horizontal resolutions about of 30m.



Taylor diagrams (Taylor, 2001) were used to test the performance of the hydraulic model coupled with the different DEMs. For that the normalized standard deviation (Eq. 1), the normalized centered root mean square difference (Eq. 2) and the correlation coefficient (Eq. 3) were used.

150

$$\sigma_n = \frac{\sqrt{\frac{\sum_{i=1}^N (S_i - \bar{S})^2}{N}}}{\sigma_O} \quad (1)$$

$$E_n = \frac{\sqrt{\frac{\sum_{i=1}^N [(S_i - \bar{S}) - (O_i - \bar{O})]^2}{N}}}{\sigma_O} \quad (2)$$

$$R = \frac{\sum_{i=1}^N [(S_i - \bar{S})(O_i - \bar{O})]}{N \sigma_S \sigma_O} \quad (3)$$

155 where S is the simulated water level obtained with the numerical model, O is the observed water level, *barred variables* refer to mean values, N is the total number of observed data, subscript i refers to the different points of available data, subscript n refers to normalized values, and σ is the standard deviation.

4 Results and Discussion

4.1 Validation of different DEMs

160 Unlike other countries such as Spain, Portugal has only free available high resolution Digital Elevation Models (DEM) for the coastal area and a few additional areas (<https://www.ign.es/web/ign/portal>; <https://dados.gov.pt/pt/>). Therefore, it is no surprise that for the lower Tagus (depicted in Figure 1) a high-resolution DEM is not freely available, as these can generally only be acquired from national organizations that produce topographical and bathymetric cartography at scales compatible with local studies. This could represent a limitation to analyze in detail the flood development over concrete locations, namely within towns or villages where high resolution is necessary to adequately address the flood progress through their
165 streets. However, global DEMs can provide an adequate representability to analyze the large-scale evolution and the magnitude of flood events (Yan et al., 2013; Courty et al., 2019). Available global DEM products have spatial resolutions varying from meters to kilometers. Horizontal and vertical accuracies can also vary greatly depending on the type of topography, and they can reach tens of meters (Thompson et al., 2001; Zhang et al., 2014).

170 In this context, and considering the wide range of available DEMs it was felt necessary to evaluate the suitability of different freely available DEMs to adequately represent floods in the lower Tagus valley. To achieve this goal, one of the most important flood events occurred in that area on February 1979, was analyzed in order to test which DEM is most appropriate



for the area under scope. Four DEMs were tested, namely ESRI, ASTER, SRTM and Copernicus DEM (Karlsson and Arnberg, 2011; Wang et al., 2012; Garrote, 2022).

175 SNIRH database provides data on the maximum water level reached during this event at some points located throughout the area under scope (see black circles in Figure 1). This information was used to perform the analysis. For that, maximum water levels reached at these control points were also extracted for the simulation carried out with each DEM. Thus, real maximum water level was compared with water level obtained in each simulation performed using the different DEMs under analysis. To analyze the performance of model results Taylor diagrams were used (Taylor, 2001) (Figure 2). The results obtained with Copernicus DEM are clearly the closest to the reference data, indicating that Copernicus DEM presents the best accuracy, 180 i.e. the best capability to address floods in the area under scope. In particular, it presents a high correlation with the measured data, above 0.99, with a normalized standard deviation close to 1 and the lowest RMSD. In addition, when the original elevation data from these DEMs are compared with the official altimetric values (see Table S2 in the Supplementary Material), Copernicus DEM is also corroborated as the most accurate (see the detailed analysis provided in the Supplementary Material). Recent studies comparing the accuracy of different DEMs along the European continent (Guth and 185 Geoffroy, 2021) and in other parts of the world (Garrote, 2022), also confirm the higher precision of Copernicus DEM in comparison with other global products.

This confirms that Copernicus DEM, coupled with the Iber+ model, are capable of the adequate reproduction, at large-scale, of the flood events in the lower Tagus. Therefore, Copernicus DEM was selected for the remaining of the analysis.

4.2 Flood event of 1979

190 This event was simulated (*Simulation_Control_1979*) in order to analyze the spatial-temporal evolution of the flood (Figure 3). In general terms, previous studies detected that the high precipitation rates that occurred during the event and the previous days caused an increase in the Tagus river flow until it reached a relative maximum surpassing $5000 \text{ m}^3\text{s}^{-1}$ at Almourol on February 5, an amount that has been associated to the beginning of the significant impacts by flood (Zêzere et al., 2014; Rebelo et al., 2018). As it can be observed in Figure 3a, the simulation indicates that a large part of the valley is 195 flooded under these conditions, although the water depth values are relatively low near the villages. On the following days, river flow experienced a certain decrease, and consequently, the simulation shows a decreasing water depth, with water slightly receding from some locations (Figure 3b). However, the situation degrades again afterwards and starts to be critical from February 9 on, reaching an outstanding maximum around February 11, surpassing $13000 \text{ m}^3\text{s}^{-1}$ at Almourol. Under these conditions most of the valley is flooded but the most important fact detected by the simulation is that the water depth 200 reveals a significant increase (Figure 3c). The high water levels reached near the villages in the simulation are a clear indication that they were affected by the flood, as confirmed by previous studies (Zêzere et al., 2014; Rebelo et al., 2018). These publications corroborate the flood impact on several important villages located in the valley, including V. N. da Barquinha, Golegã, Chamusca, Santarém, and Vila Franca de Xira (Figure 1). As commented above, the resolution of the



available DEMs does not allow resolving the entire topographic characteristics of the villages, however results obtained by
205 the simulation support the flood of these locations. In addition, previous analysis showed that these high water levels
implicated the isolation of some of these village populations and, in several occasions people had to be evacuated by boats
and helicopters since roads or railroads were waterlogged (Zêzere et al., 2014; Rebelo et al., 2018). Although these structures
usually present a certain elevation in respect to the surrounding terrain, the water depths reached during this event implicated
that they were equally flooded (Rebelo et al., 2018). Overall, the reports of flooded locations and specific sites are supported
210 by the model results. In particular, the simulation indicates an increase in the water level of the Tagus River in Santarem
above 4 meters respect to the non-flood situation, a similar increase detected with the measured data (Rebelo et al., 2018),
stressing the unusual level of this flood event. Although the river flow decreased in the following days, the flood situation
still lasted. Our simulation indicates that, on February 16 (Figure 3d), although water levels suffer an important decrease, and
water recedes from some locations of the valley, a large fraction of the valley remained flooded.

215 There are some documents that collect detailed information related to the maximum water depths reached during this flood,
constituting a valuable additional source of data useful to validate the accuracy of the model. First of all, the Portuguese
National Civil Engineering Laboratory (LNEC) and Water Institute (INAG) reconstructed the maximum flooding area
during this event (Figure 4, white line). As can be observed in Figure 4, simulated flood extension is practically coincident
with the registered flood extension. Only in the areas inside the towns, flood extension provided by the simulation is a little
220 smaller due to the limitations of the DEM commented above for which the advance of water in towns is limited.

More specifically, Rebelo et al. (2018) stated that the railroad line near to Golegã was flooded and important means of
transport were interrupted. As it can be observed in Figure 5a, the simulation detected that this infrastructure was flooded
over a large section, corroborating the blocking of the railroad. Another location with valuable information of the flood is the
town of Benfica do Ribatejo. In particular, some photographs warrant the flood of the football field of this location, situation
225 also reproduced in the model (Figure 5b). In the surroundings of Santarem, specifically in the statue dedicated to Santa Iria
(Figure 5c), there is information about the depth reached by water during this event. The existing documents indicate that
water almost reached the feet of the statue (Loureiro, 2007), which indicate a water depth about of 3m. In the model
simulation water also reaches this area (Figure 5c), with water depths surpassing the 2.5m, which is in good accordance with
real situation. Additionally, Figure 5d represents Palhota town. In this location there are several water marks in different
230 houses indicating an approximate water depth of 1.8 meters. In the simulation this town is also affected by floods, as can be
detected in Figure 5d, with a water depth ranging between 1 and 2 meters in the surrounding of this area, in line with the *in
situ* measurements. This larger range of values reflects the particular location of this water mark, inside the town where the
global DEM presents higher uncertainty. Therefore, it can be concluded that the simulations carried out in this work, using
Iber+ model in combination with Copernicus DEM, allow a good reproduction of the 1979 flood extent and water depth in
235 the lower Tagus valley.



4.3 Mitigation of Tagus floods

Tagus dams can play a key role in the mitigation of floods in the lower Tagus valley due to their high storage capacity (Rebelo et al., 2018). In particular, Alcántara dam has the greatest regulation capacity by far, as commented above, and therefore, the evaluation of possible flood mitigation in the lower Tagus by dams will be focused on Alcántara functioning.

240 In the extreme event of the 1979 flood, a relatively poor coordination and operation between Spanish and Portuguese authorities led to poor performance of dams control in terms of prevention and mitigation of the 1979 flood. When flow peaks arrived, dams controlling Tagus flow and a main tributary were virtually full therefore hampering the capacity to exert sufficient control on the peak river flow (Rebelo et al., 2018).

4.3.1 The role of Alcántara dam in lower Tagus valley

245 In order to better know the impact of the very large Alcántara dam release in the lower Tagus valley, a comparison between dam outflow and river flow reaching Almourol was established. It was detected that, for the common period of available data (1973-2018), Alcántara provides, on average, the 59.60% of water reaching Almourol. In terms of flood analysis, and taking into account that Tagus starts to overflow in its lower valley when it exceeds approximately $1500 \text{ m}^3\text{s}^{-1}$ (Ramos and Reis, 2001; Rebelo et al., 2018), this means that a dam release of approximately $1000 \text{ m}^3\text{s}^{-1}$ would imply a flood risk situation.

250 Therefore, we will consider a flood flow at Alcántara dam when the outflow exceeds $1000 \text{ m}^3\text{s}^{-1}$. Obviously, this is a general approximation since the instantaneous flow that reaches the lower Tagus valley depends on the particular conditions downstream, and therefore, the percentage of contribution from Alcántara dam can fluctuate over time. However, the present approach, considering the flow of Alcántara as 60% of the total flow that reaches the lower Tagus valley, will be used to analyze the dam functioning in a general way.

255 4.3.2 General approach to an optimal dam operating strategy

Firstly, a general analysis of historical functioning of Alcántara dam in relation to floods was carried out. The number of days with outflows with high probability of causing flooding downstream ($> 1000 \text{ m}^3\text{s}^{-1}$) was evaluated considering three different outflow strategies: i) the inflow, which represents the Tagus River in natural regime; ii) the real dam outflow, which corresponds to what really happened; iii) a controlled outflow for dam operating focused on mitigating floods keeping

260 a water storage similar to the historical one. It is important to consider that dams are multi-purpose water resource systems, and a balance should be struck between ensuring flood mitigation and other purposes, such as water supply or hydropower production (Lee et al., 2009) and, hence, the need to maintain a storage similar to the real one must be equally considered. In fact, previous studies also highlight the need to maintain dam volume conditions similar to the real ones in order to develop useful dam operating strategies (Shrestha and Kawasaki, 2020). In this sense, Alcántara dam had a mean annual volume of

265 62 % during the available data period (1970-2018), slightly lower (59 % on average) during the rainy season (from November to March). In this context, to maintain this dam filling level around 60% seems a good compromise and does not



undermine the normal operability of the dam. Therefore, dam level remains at 60% occupancy as long as river flow allows it. Thus, the proposal is based on two principles: i) to maintain a dam fill level that allows a certain free dam capacity to deal with peak flows, whenever possible, hereafter referred to base filling level (BFL); ii) the maximum outflow will be limited to 1000 m³s⁻¹ whenever allowed by dam capacity. This value corresponds to the security outflow level considered, that is an outflow below the threshold that the downstream channel is capable of safely conveying. Similar approaches have been used by previous studies developing dam release rules based on safe flow limits (e.g. Lei et al., 2020). Previous studies focused on the development of dam operating rules for flood mitigation also applied other approaches, e.g. based on algorithms to minimize peaks (Chou and Wu, 2015), neural networks (Hasebe and Nagayama, 2002), or even in dam gates functioning (Hardesty et al., 2018; Ridolfi et al., 2019). Nevertheless, other works based on principles similar to those considered here also showed a high efficiency to mitigate floods by dam operating (Lei et al., 2018; Shrestha and Kawasaki, 2020).

The dam operation under the approach rules defined above was carried out starting in October 1970 and extended to the entire available period forced with the real inflow. Thus, dam volume will vary according to the differences between inflow and outflow. Controlled outflow is obtained by means of the following equation:

$$Q_o = \begin{cases} 0 & \text{if } V_{d-1} < V_{60} \\ Q_l & \text{if } V_{60} < V_{d-1} < V_T \\ \max[Q_l, Q_i] & \text{if } V_{d-1} + V_i \geq V_T \end{cases} \quad (4)$$

where Q_o is the controlled outflow, Q_l is the security outflow level (1000 m³s⁻¹), Q_i is the river inflow, V_i is the inflow volume, V_{d-1} is the dam volume of the previous day, V_T is the total capacity of the dam and $V_{60} = 0.6 \times V_T$ (corresponding to BFL = 60%). The overall approach used here corresponds to the Operational Strategy 1 (OS1 from now on).

The results of the three approaches, natural regime, real dam outflow and controlled outflow by the dam operating proposed, are summarized in Table 1. Considering a natural regime, Tagus river flow at Alcántara higher than the considered security level was observed 456 days (average of 2.6 days per year). The actual dam regulation over these years promoted an important reduction in these risk flows, with 43 % less of cases, with a total number of 260 (1.5 days per year). The reduction in risk flows achieved with the OS1 strategy is much higher, with a total of number of days under flood conditions of 78 (0.4 days per year), i.e. a decrease of 83 % in the number of cases compared to the corresponding number for natural flow. In addition, OS1 also provides an effective reduction of the most critical river flows, reducing by 57 % the likelihood of cases in which the daily flows are exceed 3000 m³s⁻¹ and by 62 % those days with flows greater than 5000 m³s⁻¹. Thus, under the OS1, the mean dam volume along the simulation is practically the same as in the reality, but the number of floods decreases considerably.

Having demonstrated the soundness of OS1 in decreasing the number of days under flood flow conditions, the question that remains is whether that approach is sufficient to prevent flooding in the most extreme cases. In order to evaluate this under



295 different meteorological and hydrological conditions five extreme cases were selected according to literature and to the available data series (<http://www.cedex.es/>): February 1972, March 1978, February 1979, December 1989 and November 1997. All these five cases are characterized by peak flows higher than $5000 \text{ m}^3\text{s}^{-1}$ at Alcántara location. In addition, most of them are also included in the top 10 rank of the most important extreme events in terms of daily and accumulated precipitation considering the entire Tagus basin (Ramos et al., 2014; 2017).

300 The inflow and the controlled outflow (following OS1) are represented in Figure 6 for the five cases under study. Although, the number of days under flood conditions is significantly reduced for the extreme events analyzed, (7(0), 16(7), 28(11), 27(13), 27(0)), extreme flood conditions are not completely prevented. In the events with higher river flows that persists for several days, the most extreme peak flows are not smoothed, as observed in the cases of the events in 1978, 1979 and 1989. Therefore, an improvement is needed to also address these most extreme cases.

305 4.3.3 Improved approach to an optimal dam operating strategy for extreme events

Considering as a benchmark the flood that occurred in 1979, it can be observed that with the application of the OS1, the simulated outflow coincides with the natural regime for the maximum peak flow, as well as for the high river discharges that occurred the previous and the following day (Figure 6, third panel), indicating that the dam was full. An efficient approach mostly focused on minimizing the effects of these extreme peak flows could be to allow higher outflows, above $1000 \text{ m}^3\text{s}^{-1}$,
 310 in the previous days, guaranteeing a sufficient dam free volume to minimize the extreme peaks, which would result in producing controlled floods. However, it is important to take into account that the outflow must always be limited by the inflow when it exceeds the safety flow, that is, the outflow can never exceed the inflow under flood conditions. This allows reducing the extreme peaks but avoiding inducing man-made floods, an approach also considered fundamental in previous studies addressing dam operation to mitigate floods (Chou and Wu, 2015). To achieve this goal, a second approach was
 315 added to the strategy presented above to deal with extreme flow situations. Analyzing the existing data, it will only be necessary to apply this approach for the most extreme events, that is, when the expected accumulated volume for the following 7 days exceeds the 99.9th percentile of the historical series. Under this conditions, controlled outflow is obtained by means of the following equation:

$$Q_o = \begin{cases} 0 & \text{if } V_{d-1} + V_i < V_{60} \\ Q_l & \text{if } V_{60} < V_{d-1} + V_i < V_{80} \\ \max[Q_l, \min(Q_{o80}, Q_i)] & \text{if } V_{80} < V_{d-1} + V_i < V_T \text{ and } V_i \neq V_{max} \\ \max[Q_l, \min(Q_{o100}, Q_i)] & \text{if } V_{80} < V_{d-1} + V_i < V_T \text{ and } V_i = V_{max} \\ & \text{or } V_{d-1} + V_i > V_T \end{cases} \quad (5)$$

320 V_{80} is the volume considered as the security Base Filling Level for extreme events, considered as 80% of dam capacity ($V_{80} = 0.8 \times V_T$). V_{max} is referred to the day when the peak of the event is expected. $Q_{o80} = Q_i + V_{d-1} - V_{80}$ is the



outflow which allows maintaining the volume of the dam at 80% of its capacity and $Q_{o100} = Q_i + V_{d-1} - V_T$ is the outflow that allows not to exceed the dam capacity. The overall approach used here corresponds to the Operational Strategy 2 (OS2 from now on).

- 325 To apply this strategy, it is also necessary to know in an approximate way the expected volume for the following days, in order to detect possible extreme situations, however the uncertainty associated to strategies based on more precise forecasts is reduced. Thus, the present condition is focused in guaranteeing a certain free reservoir capacity to smooth the most extreme peak flows, so it will only be applied in very extreme conditions, since the necessary condition to be applied is highly restrictive. In the rest of the cases, OS1 would be applied.
- 330 Table 2 shows the main characteristics of the controlled dam outflow applying this new configuration for the extreme cases. It can be noticed that the main peak flow is reduced by more than 35% in the 1979 flood event. An important reduction also occurred in the other extreme cases equally not smoothed with OS1: the peak flow of the 1978 flood event is reduced by about 30 %, and the peak of the 1989 extreme event is reduced by about 40 %.

4.3.4 Hydraulic analysis of the effectiveness of the dam operating strategy in relation to flood mitigation

- 335 It is important to take into account that although the peaks are reduced applying the OS2, the total multi-day outflow volume throughout the events is similar (within each event) for the dam operations considered. Therefore, taking into account the flattened shape of the valley, which implies that a large area can be flooded, even with relatively lower flows as it was detected in Figure 3, it is crucial to assess what both approaches imply in terms of effective flooding reduction in lower Tagus valley. This issue can be addressed again taking advantage of the Iber+ hydraulic model. Therefore, three simulations
- 340 (*Simulation_Dam*) were performed for each extreme event, that is, considering outflow at Alcántara corresponding to: i) natural regime, ii) OS1; iii) OS2. In order to keep the analysis within a manageable size we restrict the full assessment to the flood event of 1979 considered as benchmark, where Figure 7a shows the natural river flow and the controlled outflow of the dam obtained by applying the new configuration (OS2). In addition of the reduction of maximum amplitude, the peak flow is delayed by one day, which can further decrease flood damage downstream. To evaluate the real reduction on flooding in
- 345 lower Tagus valley for the event of 1979 under the different strategies presented, the simulated maximum flood caused by the Alcántara outflow resulting from natural regime and operating strategy OS2 is shown in Figures 7b and 7c, respectively. The most important fact is that the entire area presents an important reduction in water depth under the most effective dam operating strategy. This reduction is shown in more detail in Figure 8 where the differences between both cases are highlighted, with a decrease that can surpass one meter in some locations. In addition, although the reduction in flood
- 350 extension is small compared to the total extension of the valley, it can be detected as water is also retracted at some extent in the surroundings of the villages (see zoomed areas in Figure 8). Therefore, the application of the OS2 could suppose an important flood alleviation for the area under scope.



This flood mitigation analysis was also applied for the rest of the extreme events, in order to provide information focused on effective mitigation measures and to understand their impact on flood reduction. For that, the floods caused by the different configurations, that is, the natural flow regime and the operating strategies OS1 and OS2, were analyzed and compared for the most critical events by means of the respective hydraulic simulations (Table 3). This allows to extract key information for the area under scope. As commented above, the events occurred in 1972 and 1997 can be completely avoided at Alcántara location, therefore the analysis will be focused on the rest of the extreme events. According to hydraulic simulations, in these most extreme events is not possible to prevent most of the valley from being flooded even with dam regulation presented in OS2. This is mainly due to the flattened shape of the valley, which favors flooding even with lower discharges, as detected in Figure 3. Specifically, a reduction of around 5-10% in the total extension of the flood is achieved on average in the most extreme cases (from 565 km² to 531 km² in the 1979 flood event). Once most of the valley is flooded, the main increase occurs in terms of water depth. This is a critical and dangerous factor, since the damages caused by floods are closely linked to the water depths reached (Tsakiris, 2014; Huizinga et al., 2017). In this sense, the mitigation of floods in the lower Tagus valley allowed by an efficient regulation of dams, is especially effective in terms of water depth reduction (Table 3). On average, OS2 allows reducing water depths in flooded areas by more than 0.5 m, which supposes a reduction of around 25 % in water depth. In the particular case of the 1979 flood, the average maximum water depth is reduced from 2.57 m to 1.88 m. This contributes to a significant reduction in flood damages and the associated costs, which are proportional to the water depths (Huizinga et al., 2017). Another important aspect that should be taken into account to assess flood damages is the maximum velocity reached by water (Cox et al., 2011). In this sense, the presented strategy also contributed to a reduction in this flood hazard metric, reducing the maximum velocity reached by the water in the flooded areas by around 25-30 % (Table 3). In particular, the average maximum velocity of the water in flooded areas is reduced from 0.51 ms⁻¹ to 0.36 ms⁻¹ in the 1979 flood.

The results obtained corroborate the important mitigation of flood impacts that can be achieved in the lower Tagus basin taking advantage of the existing dam capacity.

5 Conclusions

This work aimed to present a strategy that allows taking advantage of the existing dams in the Tagus river to effectively mitigate the most extreme floods, that have occurred in its lower valley in recent decades, and may occur again in the future. For this, a dam operating strategy was developed in combination with the Iber+ hydraulic model to analyze the effectiveness of the proposal in relation to flood mitigation.

Firstly, Iber+ model was validated for the area under scope. Several DEMs were used to determine the best one to macroscopically reproduce the floods in the lower Tagus valley. Copernicus DEM shows the best accuracy. In fact, Iber+



385 model coupled with Copernicus DEM was able to provide an adequate macroscopic reproduction of the most important
flood of the last 150 years in the Tagus valley, the 1979 flood, which demonstrates its capability to evaluate floods in the
area under study and allows the hydrodynamic analysis of this event.

Once the Iber+ model was validated, the analysis was focused on developing dam operating strategies to help in flood
mitigation. Specifically, the analysis was focused on Alcántara dam, the most important on the Tagus river. In general terms,
results indicate that the proposed strategy allows diminishing the number of days under flood conditions by more than 80 %
390 with respect to the natural regime, and an important reduction is also obtained in relation to the historical dam operation. In
addition, the mitigation of the most extreme flood events was also achieved. Hydraulic simulations confirm that the proposed
operating strategy is especially effective in reducing water depth and water velocity in the flooded areas (~ 25-30 %), the
most critical factors in terms of flood damage. In addition, a smaller reduction in flood extension is also achieved (~ 5-10
%). Therefore, hydraulic simulations corroborate the significant flood mitigation in the lower Tagus valley that can be
395 achieved with more appropriate use of dam strategies, as proposed in this work. This demonstrates the effectiveness of the
strategies proposed to address the future implications of the climate change in relation to the expected more frequent and
intense flood events in the future.

We acknowledge that our work has some caveats, namely the relatively low resolution of our DEM, specially over
constructed areas that have been flooded and where a more detailed analysis requires a higher resolution DEM such as the
400 DEM produced and made available by the Direção Geral do Território (DGT), which corresponds to a strip of 600 m at sea
and 400 m on land, of the coastal areas of mainland Portugal with a resolution of 2 m, obtained from a survey with LiDAR
technology. An equivalent DEM, but for all continental territory, was already announced in 2021 by DGT, although it is not
yet available at the time of this study. In addition, although the DEM used appears to provide an adequate macroscopy view
of the flood and allows for a general analysis of flood mitigation under the different dam strategies presented, the absolute
405 values obtained in some locations should be taken with caution for the reasons commented above.

This study can be viewed as a first step to improve the knowledge on extreme floods in the lower Tagus valley and to
provide strategies to mitigate these events taking advantage of the existing infrastructures, thus addressing one of the most
important challenges that the scientific community will have to face in the coming decades as a consequence of climate
change. Future improvements should be focused on the integration of the dam operating strategies for real-time early
410 warning systems, which, in combination with the hydraulic models and good weather forecasts, will allow evaluating in
advance the possible flood scenarios and apply the right measures that minimize the floods (Chang et al., 2010; Chou and
Wu, 2015; Fakhruddin et al., 2015; Fraga et al., 2020). This will also allow to improve and make more precise the dam
strategies applied. As commented above, a future improvement and development of high resolution DEMs for the area under
scope will be also necessary to enable more detailed analysis of flooding within the villages which will allow to the local
415 authorities to take adequate and more precise measures to mitigate flood damage.



Code and data availability: Freely available data and software were used for this work.

420

Author contribution: DFN: Conceptualization, Methodology, Formal analysis, Investigation, Writing – Original Draft. AMR: Methodology, Investigation, Writing – Review & Editing. JGC: Methodology, Investigation, Writing – Review & Editing. OGF: Methodology, Investigation, Writing – Review & Editing. CC: Methodology, Investigation, Writing – Review & Editing. MGG: Conceptualization, Methodology, Writing – Review & Editing, Supervision. RMT: Conceptualization,
425 Methodology, Writing – Review & Editing, Supervision.

Competing interests: The authors declare that they have no conflict interest.

430 **Acknowledgements**

The authors thank the “Sistema Nacional de Informação de Recursos Hídricos” (SNIRH), the Centro de Estudios y Experimentación de Obras Públicas (CEDEX), and the developers of Iberia01 database for the information provided for this work.

This work was partially supported by Xunta de Galicia, Consellería de Cultura, Educación e Universidade, under Project
435 ED431C 2021/44 “Programa de Consolidación e Estructuración de Unidades de Investigación Competitivas”. AMR, CC and RT were partially supported by EEA-Financial Mechanism 2014-2021 and the Portuguese Environment Agency through Pre-defined Project-2 National Roadmap for Adaptation XXI (PDP-2).

DFN was supported by Xunta de Galicia through a post-doctoral grant (ED481B-2021-108). AMR was supported by the Scientific Employment Stimulus 2017 from FCT (CEECIND/00027/2017). OGF was funded by Spanish “Ministerio de
440 Universidades” and European Union – NextGenerationEU through the “Margarita Salas” post-doctoral grant.

References

Agência Portuguesa do Ambiente, Plano De Gestão De Região Hidrográfica. Parte 2 – Caracterização E Diagnóstico. Região Hidrográfica Do Tejo e Ribeiras do Oeste (RH5), 2016. Agência Portuguesa do Ambiente. Ministério do Ambiente e da Transição Energética, Lisboa, Portugal.
445



- Alfieri, L., Burek, P., Feyen, L., and Forzieri, G.: Global warming increases the frequency of river floods in Europe, *Hydrol. Earth Syst. Sc.*, 19(5), 2247-2260, <https://doi.org/10.5194/hess-19-2247-2015>, 2015.
- Alfieri, L., Bisselink, B., Dottori, F., Naumann, G., de Roo, A., Salamon, P., Wyser, K., and Feyen, L.: Global projections of river flood risk in a warmer world, *Earth's Future*, 5, 171–182. <https://doi.org/10.1002/2016EF000485>, 2017.
- 450 Arnell, N. W., and Gosling, S. N.: The impacts of climate change on river flood risk at the global scale, *Clim. Change*, 134(3), 387-401, <https://doi.org/10.1007/s10584-014-1084-5>, 2016.
- Becek, K., Koppe, W., and Kutoğlu, Ş. H.: Evaluation of vertical accuracy of the WorldDEM™ using the runway method, *Remote Sensing*, 8(11), 934, <https://doi.org/10.3390/rs8110934>, 2016.
- Benito, G., Machado, M. J., and Pérez González, A.: Climate change and flood sensitivity in Spain, En: Brandson, J., Brown, A. G. y Gregory, K. L. (Eds). *Global continental Changes: the context of palaeohydrology*. Geological Society Special Publication n° 115, 85-98. Londres. 1996.
- 455 Benito, G., Díez-Herrero, A., and de Villalta, M.: Magnitude and frequency of flooding in the Tagus Basin (Central Spain) over the last millennium, *Clim. Change*, 58, 171-192, 2003.
- Bermúdez, M., Farfán, J. F., Willems, P., and Cea, L.: Assessing the Effects of Climate Change on Compound Flooding in Coastal River Areas, *Water Resour. Res.*, 57 (10), e2020WR029321, <https://doi.org/10.1029/2020WR029321>, 2021.
- 460 Bladé, E., Cea, L., Corestein, G., Escolano, E., Puertas, J., Vázquez-Cendón, E., Dolz, J., and Coll, A.: Iber - River modelling simulation tool [Iber: herramienta de simulación numérica del flujo en ríos], *Revista Internacional de Metodos Numericos para Calculo y Diseno en Ingenieria*, 30 (1), 1-10. <https://doi.org/10.1016/j.rimni.2012.07.004>, 2014.
- 465 Bonasia, R., and Ceragene, M.: Hydraulic numerical simulations of La Sabana river floodplain, Mexico, as a tool for a flood terrain response analysis, *Water*, 13 (24), 3516, <https://doi.org/10.3390/w13243516>, 2021.
- Carrera-Hernandez, J. J.: Not all DEMs are equal: An evaluation of six globally available 30 m resolution DEMs with geodetic benchmarks and LiDAR in Mexico, *Remote Sens. Environ.*, 261, 112474, <https://doi.org/10.1016/j.rse.2021.112474>, 2021.
- 470 Chang, L. C., Chang, F. J., and Hsu, H. C.: Real-time reservoir operation for flood control using artificial intelligent techniques, *Int. J. Nonlin. Sci. Num.*, 11(11), 887-902, <https://doi.org/10.1515/IJNSNS.2010.11.11.887>, 2010.
- Chou, F. N. F., and Wu, C. W.: Stage-wise optimizing operating rules for flood control in a multi-purpose reservoir, *J. Hydrol.*, 521, 245-260, <https://doi.org/10.1016/j.jhydrol.2014.11.073>, 2015.
- CLC. European Union, Copernicus Land Monitoring Service 2000, European Environment Agency (EEA).
- 475 Courty, L. G., Soriano-Monzalvo, J. C., and Pedrozo-Acuña, A.: Evaluation of open-access global digital elevation models (AW3D30, SRTM, and ASTER) for flood modelling purposes, *J. Flood Risk Manag.*, 12, e12550, <https://doi.org/10.1111/jfr3.12550>, 2019.
- Cox, R. J., Shand, T. D., and Blacka, M. J.: Australian Rainfall and Runoff revision project 10: appropriate safety criteria for people. Water Research Laboratory, P10/S1/006. 2010.



- 480 Dankers, R., and Feyen, L.: Climate change impact on flood hazard in Europe: An assessment based on high-resolution climate simulations, *J. Geophys. Res.-Atmos.*, 113(D19), <https://doi.org/10.1029/2007JD009719>, 2008.
- Diakakis, M.: Have flood mortality qualitative characteristics changed during the last decades? The case study of Greece, *Environmental Hazards*, 15(2), 148-159, <https://doi.org/10.1080/17477891.2016.1147412>, 2016.
- Fakhruddin, S. H. M., Kawasaki, A., and Babel, M. S.: Community responses to flood early warning system: Case study in
485 Kaijuri Union, Bangladesh, *Int. J. Disast. Risk Re.*, 14, 323-331, <https://doi.org/10.1016/j.ijdr.2015.08.004>, 2015.
- Fernández-Nóvoa, D., deCastro, M., Des, M., Costoya, X., Mendes, R., and Gómez-Gesteira, M.: Characterization of Iberian turbid plumes by means of synoptic patterns obtained through MODIS imagery, *J. Sea Res.*, 126, 12-25, <https://doi.org/10.1016/j.seares.2017.06.013>, 2017.
- Fernández-Nóvoa, D., García-Feal, O., González-Cao, J., de Gonzalo, C., Rodríguez-Suárez, J. A., Ruiz del Portal, C., and
490 Gómez Gesteira, M.: MIDAS: A New Integrated Flood Early Warning System for the Miño River, *Water*, 12, 2319, <https://doi.org/10.3390/w12092319>, 2020.
- Fraga, I., Cea, L., and Puertas, J.: MERLIN: a flood hazard forecasting system for coastal river reaches, *Nat. Hazards*, 100 (3), 1171–1193. <https://doi.org/10.3390/w12092319>, 2020.
- García-Feal, O., González-Cao, J., Gomez-Gesteira, M., Cea, L., Domínguez, J. M., and Formella, A.: An accelerated tool
495 for flood modelling based on Iber, *Water* 10 (10), 1459, <https://doi.org/10.3390/w10101459>, 2018.
- Garrote, J.: Free Global DEMs and Flood Modelling—A Comparison Analysis for the January 2015 Flooding Event in Mocuba City (Mozambique), *Water*, 14(2), 176, <https://doi.org/10.3390/w14020176>, 2022.
- González-Cao, J., Fernández-Nóvoa, D., García-Feal, O., Figueira, J. R., Vaquero, J. M., Trigo, R. M., and Gómez-Gesteira, M.: The Rivillas flood of 5–6 November 1997 (Badajoz, Spain) revisited: An approach based on Iber+ modelling, *J.*
500 *Hydrol.*, 610, 127883, <https://doi.org/10.1016/j.jhydrol.2022.127883>, 2022.
- González-Cao, J., Fernández-Nóvoa, D., García-Feal, O., Figueira, J. R., Vaquero, J. M., Trigo, R. M., and Gómez-Gesteira, M.: Numerical reconstruction of historical extreme floods: The Guadiana event of 1876, *J. Hydrol.*, 599, 126292, <https://doi.org/10.1016/j.jhydrol.2021.126292>, 2021.
- González-Cao, J., García-Feal, O., Fernández-Nóvoa, D., Domínguez-Alonso, J. M., and Gómez-Gesteira, M.: Towards an
505 automatic early warning system of flood hazards based on precipitation forecast: the case of the Miño River (NW Spain), *Nat. Hazard Earth Sys.*, 19, 2583-2595, <https://doi.org/10.5194/nhess-19-2583-2019>, 2019.
- Guth, P. L., and Geoffroy, T. M.: LiDAR point cloud and ICESat-2 evaluation of 1 second global digital elevation models: Copernicus wins, *Transactions in GIS*, 25, 2245-2261, <https://doi.org/10.1111/tgis.12825>, 2021.
- Hardesty, S., Shen, X., Nikolopoulos, E., and Anagnostou, E.: A numerical framework for evaluating flood inundation
510 hazard under different dam operation scenarios—A case study in Naugatuck river, *Water*, 10(12), 1798, <https://doi.org/10.3390/w10121798>, 2018.
- Hasebe, M., and Nagayama, Y.: Reservoir operation using the neural network and fuzzy systems for dam control and operation support, *Adv. Eng. Softw.*, 33(5), 245-260, [https://doi.org/10.1016/S0965-9978\(02\)00015-7](https://doi.org/10.1016/S0965-9978(02)00015-7), 2002.



- Herrera, S., Cardoso, R. M., Soares, P. M. M., Espírio-Santo, F., Viterbo, P., and Gutiérrez, J. M.: Iberia01: Daily gridded
515 (0.1° resolution) dataset of precipitation and temperatures over the Iberian Peninsula. DIGITAL.CSIC,
<http://dx.doi.org/10.20350/digitalCSIC/8641>, 2019.
- Huizinga, J., De Moel, H., and Szewczyk, W.: Global flood depth-damage functions: Methodology and the database with
guidelines. Joint Research Centre, JRC105688, (Seville site), 2017.
- IPCC, 2012. Managing the Risks of Extreme Events and Disasters to Advance Climate Change Adaptation. A Special Report
520 of Working Groups I and II of the Intergovernmental Panel on Climate Change [Field, C.B., Barros, V., Stocker,
T.F., Qin, D., Dokken, D.J., Ebi, K.L., Mastrandrea, M.D., Mach, K.J., Plattner, G.-K., Allen, S.K., Tignor, M.,
Midgley, P.M. (eds.)]. Cambridge University Press, Cambridge, UK, and New York, NY, USA, 582 pp.
- IPCC, 2021: Climate Change 2021: The Physical Science Basis. Contribution of Working Group I to the Sixth Assessment
525 Report of the Intergovernmental Panel on Climate Change [Masson-Delmotte, V., P. Zhai, A. Pirani, S.L. Connors,
C. Péan, S. Berger, N. Caud, Y. Chen, L. Goldfarb, M.I. Gomis, M. Huang, K. Leitzell, E. Lonnoy, J.B.R.
Matthews, T.K. Maycock, T. Waterfield, O. Yelekçi, R. Yu, and B. Zhou (eds.)]. Cambridge University Press,
Cambridge, United Kingdom and New York, NY, USA.
- Jaafar, H. H., Ahmad, F. A., and El Beyrouthy, M.: GCN250, new global gridded curve numbers for hydrologic modeling
and design. Scientific data 6, 1-9. <http://dx.doi.org/10.1038/s41597-019-0155-x>, 2019.
- 530 Jongman, B.: Effective adaptation to rising flood risk. Nat. Commun., 9(1), 1-3, <http://dx.doi.org/10.1038/s41467-018-04396-1>, 2018.
- Karlsson, J.M., and Arnberg, W.: Quality analysis of SRTM and HYDRO1K: a case study of flood inundation in
Mozambique, Int. J. Remote Sens., 32(1), 267-285, <https://doi.org/10.1080/01431160903464112>, 2011.
- Lee, S. Y., Hamlet, A. F., Fitzgerald, C. J., and Burges, S. J.: Optimized flood control in the Columbia River Basin for a
535 global warming scenario, J. Water Res. Plan. Man., 135(6), 440-450, 2009.
- Lei, X., Zhang, J., Wang, H., Wang, M., Khu, S. T., Li, Z., and Tan, Q.: Deriving mixed reservoir operating rules for flood
control based on weighted non-dominated sorting genetic algorithm II, J. Hydrol., 564, 967-983,
<https://doi.org/10.1016/j.jhydrol.2018.07.075>, 2018.
- Lopes, C. L., Sousa, M. C., and Ribeiro, A.: Evaluation of future estuarine floods in a sea level rise context, Sci. Rep., 12,
540 8083, <https://doi.org/10.1038/s41598-022-12122-7>, 2022.
- Lorenzo, M. N., and Alvarez, I.: Climate change patterns in precipitation over Spain using CORDEX projections for 2021–
2050, Sci. Total Environ., 723, 138024, <https://doi.org/10.1016/j.scitotenv.2020.138024>, 2020.
- Loureiro, J. M.: Rio Tejo. As Grandes Cheigas. 1800-2007, Tágides, 2007.
- Mockus, V., 1964. National engineering handbook. US Soil Conservation Service. Washington, DC, USA, 4.
- 545 Modarres, R., Sarhadi, A., and Burn, D. H.: Changes of extreme drought and flood events in Iran, Global Planet. Change,
144, 67-81, <https://doi.org/10.1016/j.gloplacha.2016.07.008>, 2016.



- Mukherjee, S., Joshi, P. K., Mukherjee, S., Ghosh, A., Garg, R. D., and Mukhopadhyay, A.: Evaluation of vertical accuracy of open source Digital Elevation Model (DEM), *Int. J. Appl. Earth Obs.*, 21, 205-217, <https://doi.org/10.1016/j.jag.2012.09.004>, 2013.
- 550 Peixoto, J. P., and Oort, A. H.: *Physics of Climate*. New York, NY: American Institute of Physics, 412–433. 1992.
- Pereira, S., Ramos, A. M., Zêzere, J. L., Trigo, R. M., and Vaquero, J. M.: Spatial impact and triggering conditions of the exceptional hydro-geomorphological event of -December 1909 in Iberia, *Nat. Hazard Earth Sys.*, 16, 371-390, <https://doi.org/10.5194/nhess-16-371-2016>, 2016.
- Petrow, T., and Merz, B.: Trends in flood magnitude, frequency and seasonality in Germany in the period 1951–2002, *J. Hydrol.*, 371(1-4), 129-141, <https://doi.org/10.1016/j.jhydrol.2009.03.024>, 2009.
- 555 Ramos, C., and Reis, E.: As cheias no Sul de Portugal em diferentes tipos de bacias hidrográficas, *Finisterra*, 36, 61-82, 2001.
- Ramos, A. M., Trigo, R. M., and Liberato, M. L.: A ranking of high-resolution daily precipitation extreme events for the Iberian Peninsula, *Atmos. Sci. Lett.*, 15(4), 328-334, <https://doi.org/10.1002/asl2.507>, 2014.
- 560 Ramos, A. M., Trigo, R. M., and Liberato, M. L.: Ranking of multi-day extreme precipitation events over the Iberian Peninsula, *Int. J. Climatol.*, 37(2), 607-620, <https://doi.org/10.1002/joc.4726>, 2017.
- Rebelo, L., Ramos, A. M., Pereira, S., and Trigo, R. M.: Meteorological Driving Mechanisms and Human Impacts of the February 1979 Extreme Hydro-Geomorphological Event in Western Iberia, *Water*, 10, 454, <https://doi.org/10.3390/w10040454>, 2018.
- 565 Ridolfi, E., Di Francesco, S., Pandolfo, C., Berni, N., Biscarini, C., and Manciola, P.: Coping with extreme events: Effect of different reservoir operation strategies on flood inundation maps, *Water*, 11(5), 982, <https://doi.org/10.3390/w11050982>, 2019.
- Rocha, C., Antunes, C., and Catita, C.: Coastal Vulnerability Assessment Due to Sea Level Rise: The Case Study of the Atlantic Coast of Mainland Portugal, *Water*, 12, 360, <https://doi.org/10.3390/w12020360>, 2020.
- 570 Salgueiro, A. R., Machado, M. J., Barriendos, M. García Perira, H., and Benito, G.: Flood magnitudes in the Tagus River (Iberian Peninsula) and its stochastic relationship with daily North Atlantic Oscillation since mid-19th Century, *J. Hydrol.*, 502, 191-201, <https://doi.org/10.1016/j.jhydrol.2013.08.008>, 2013.
- Santos, M., Fragoso, M., and Santos, J. A.: Damaging flood severity assessment in Northern Portugal over more than 150 years (1865–2016), *Nat. Hazards*, 91(3), 983-1002. <https://doi.org/10.1007/s11069-017-3166-y>, 2018.
- 575 Shrestha, B. B., and Kawasaki, A.: Quantitative assessment of flood risk with evaluation of the effectiveness of dam operation for flood control: A case of the Bago River Basin of Myanmar, *Int. J. Disast. Risk Re.*, 50, 101707, <https://doi.org/10.1016/j.ijdr.2020.101707>, 2020.
- Szabó, G., Singh, S. K., Szabó, S.: Slope angle and aspect as influencing factors on the accuracy of the SRTM and the ASTER GDEM databases, *Physics and Chemistry of the Earth, Parts A/B/C*, 83, 137-145.
- 580 <https://doi.org/10.1016/j.pce.2015.06.003>, 2015.



- Taylor, K. E.: Summarizing multiple aspects of model performance in a single diagram, *J. Geophys. Res.-Atmos.*, 106, 7183–7192, <https://doi.org/10.1029/2000JD900719>, 2001.
- Thompson, J. A., Bell, J. C., and Butler, C. A.: Digital elevation model resolution: effects on terrain attribute calculation and quantitative soil-landscape modeling, *Geoderma*, 100(1-2), 67-89. [https://doi.org/10.1016/S0016-7061\(00\)00081-1](https://doi.org/10.1016/S0016-7061(00)00081-1), 2001.
585
- Trigo, R. M., and DaCamara, C.C.: Circulation weather types and their influence on the precipitation regime in Portugal, *Int. J. Climatol.*, 20 (13), 1559-1581, [https://doi.org/10.1002/1097-0088\(20001115\)20:13<1559::AID-JOC555>3.0.CO;2-5](https://doi.org/10.1002/1097-0088(20001115)20:13<1559::AID-JOC555>3.0.CO;2-5), 2000.
- Trigo, I. F.: Climatology and interannual variability of storm-tracks in the Euro-Atlantic sector: a comparison between ERA-40 and NCEP/NCAR reanalyses, *Clim. Dyn.*, 26, 127–143, <https://doi.org/10.1007/s00382-005-0065-9>, 2006.
590
- Trigo, R. M., Varino, F., Ramos, A. M., Valente, M. A., Zêzere, J. L., Vaquero, J. M., Gouveia, C. M., and Russo, A.: The record precipitation and flood event in Iberia in December 1876: description and synoptic analysis, *Front. Earth Sci.*, 2, 3, <https://doi.org/10.3389/feart.2014.00003>, 2014.
- Tsakiris, G. J. N. H.: Flood risk assessment: concepts, modelling, applications, *Nat. Hazard Earth Sys.*, 14(5), 1361-1369, <https://doi.org/10.5194/nhess-14-1361-2014>, 2014.
595
- Valeriano, O. C. S., Koike, T., Yang, K., and Yang, D.: Optimal dam operation during flood season using a distributed hydrological model and a heuristic algorithm, *J. Hydrol. Eng.*, 15(7), 580-586, 2010.
- Vargas, I. C. C., Oliveira, S. B. F., Oliveira, A., and Charneca, N.: Análise da Vulnerabilidade de uma Praia Estuarina à Inundação: Aplicação à Restinga do Alfeite (Estuário do Tejo), *Revista da Gestão Costeira Integrada*, 8(1), 25-43, 2008.
600
- Wang, W., Yang, X., and Yao, T.: Evaluation of ASTER GDEM and SRTM and their suitability in hydraulic modelling of a glacial lake outburst flood in southeast Tibet, *Hydrol. Process.*, 26(2), 213-225, <https://doi.org/10.1002/hyp.8127>, 2012.
- Yan, K., Di Baldassarre, G., and Solomatine, D.P.: Exploring the potential of SRTM topographic data for flood inundation modelling under uncertainty. *J. Hydroinform.*, 15(3), 849-861. <https://doi.org/10.2166/hydro.2013.137>, 2013.
605
- Zêzere, J. L., Pereira, S., Tavares, A. O., Bateira, C., Trigo, R. M., Quaresma, I., Santos, P. P., Santos, M., and Verde, J.: DISASTER: A GIS database on hydro-geomorphologic disasters in Portugal, *N. Hazards*, 72, 503–532, <https://doi.org/10.1007/s11069-013-1018-y>, 2014.
- Zhang, P., Liu, R., Bao, Y., Wang, J., Yu, W., and Shen, Z.: Uncertainty of SWAT model at different DEM resolutions in a large mountainous watershed, *Water Res.*, 53, 132-144. <https://doi.org/10.1016/j.watres.2014.01.018>, 2014.
610



Table and Figure Captions

Table 1. Number of days under different critical outflows at Alcántara location considering the real inflow (natural regime), the real dam outflow, and the dam outflow under the operation strategy OS1 presented in equation 4. Percentages are referred to the differences with respect to the worst scenario (natural regime), which is assigned a percentage of 100 %.

Table 2. Hydrologic characteristic of most extreme flood events under different dam configurations. NR is referred to the natural regime (no dam), OS1 is referred to the operation strategy presented in equation (4), and OS2 is referred to the operation strategy focused on extreme events, presented in equation (5).

Table 3. Hydraulic characteristic of most extreme flood events in the lower Tagus valley considering the outflows provided by the different dam configurations considered (*Simulation_Dam*). NR is referred to the natural regime (no dam), OS1 is referred to the operation strategy presented in equation (4), and OS2 is referred to the operation strategy focused on extreme events presented in equation (5). The percentage values represent the reduction obtained with respect to the situation under natural regime. The events occurred in 1972 and 1997 were not included in the hydraulic analysis because they can be avoided at Alcántara location (see Table 2).

Figure 1. Area of study. Left panel indicates the location of the study area (dashed black rectangle) including the lower Tagus valley. Green diamond indicates the location of Almourol station and green circle indicates the location of Alcántara dam. The right panels represent the basin under scope. In the upper right panel, the black circles represent the control points where there is data on the water levels reached in the 1979 flood event. The grey triangles represent areas with relevant flood information (particular flooded areas, water depths...) for the 1979 event, from north to south: railroad of Golegã, Santa Iria statue at Santarem, football field at Benfica do Ribatejo, and Palhota town. The white circles indicate the location of the main villages affected by the flood: from north to south: V.N. da Barquinha, Golegã, Chamusca, Santarém and Vila Franca da Xira. In the lower right panel, the main locations of interest are represented. Bathymetry and topography basemaps were provided by ESRI©.

Figure 2. Taylor diagram of the water elevation obtained with Iber+ using the field data as reference. E, A, S and C indicate the Iber+ data obtained using the ESRI, ASTER, SRTM and Copernicus Digital Elevation Models.

Figure 3. Reproduction of water depth (meters) for the flood event occurred in February, 1979 in lower Tagus valley, using Iber+ hydraulic model. a), b), c) and d) represents the flood situation on 5, 8, 11 and 16 February under the *Simulation_Control_1979*.

Figure 4. Maximum flood extension for event of February, 1979, in lower Tagus, obtained from the hydraulic simulation (*Simulation_Control_1979*). The white line represents the real extension of the flood reconstructed by the National Civil Engineering Laboratory (LNEC) and the Water Institute (INAG) from Portugal (www.snirh.pt).



Figure 5. Detailed flooded area obtained with hydraulic simulation (Simulation_Control_1979) for: a) railroad of Golegã, b) football field at Benfica do Ribatejo, c) Santa Iria statue at Santarem, and d) Palhota town. The red arrow indicates the level reached by the water. The photographs and measurements in panels c) and d) were taken by the authors. Aerial maps in
645 panels a), b), c) and d) from: Map data © 2015 Google Satellite.

Figure 6. Natural regime (blue line) and simulated outflow resulting for the operation strategy OS1 of equation (4) (red line) for Alcántara dam in the most extreme cases. The date is referred to the occurrence of the highest peak flow.

Figure 7. (a) Natural regime at Alcántara (blue line) and simulated Alcántara dam outflow under the operation strategy OS2 (red line), considering the flooding of 1979. Lower panels show the maximum water depth (meters) obtained with Iber+ for
650 the outflows corresponding to (b) natural regime, and (c) dam operation strategy OS2, applied to the 1979 flood event.

Figure 8. Difference in maximum water depth (meters) caused by the Alcántara outflows corresponding to natural regime (NR) and operation strategy OS2 (OS2 – NR), applied to the 1979 flood event. Red colors represent locations reached by water under the most extreme case (NR) and not flooded when OS2 is applied. The zoomed areas show the retraction in flood extent that occurs when the most effective dam operation is applied. In particular, left zoomed area represents the
655 surroundings of Castanheira do Ribatejo town, whereas right zoomed area represents the zone delimited by the towns of Mato de Miranda, Azinhaga and Pombalinho in the surroundings of Golegã location.



Parameter	Natural Regime	Real Dam Outflow	Operation Strategy OS1
<i>Days > 1000 m³s⁻¹</i>	456 (100 %)	260 (57 %)	78 (17 %)
<i>Days > 3000 m³s⁻¹</i>	37 (100 %)	24 (65 %)	16 (43 %)
<i>Days > 5000 m³s⁻¹</i>	8 (100 %)	5 (63 %)	3 (38 %)

660 **Table 1.** Number of days under different critical outflows at Alcántara location considering the real inflow (natural regime), the real dam outflow, and the dam outflow under the operation strategy OS1 presented in equation 4. Percentages are referred to the differences with respect to the worst scenario (natural regime), which is assigned a percentage of 100 %.



Event	Flood Days			Peak Flow (m ³ s ⁻¹)		
	<i>NR</i>	<i>OS1</i>	<i>OS2</i>	<i>NR</i>	<i>OS1</i>	<i>OS2</i>
1972	7	0	0	5505	1000	1000
1978	16	7	8	7122	7122	5106
1979	28	11	15	8022	8022	5360
1989	27	13	13	5003	5003	3084
1997	27	0	0	5301	1000	1000

665 **Table 2.** Hydrologic characteristic of most extreme flood events under different dam configurations. NR is referred to the natural regime (no dam), OS1 is referred to the operation strategy presented in equation (4), and OS2 is referred to the operation strategy focused on extreme events, presented in equation (5).



Event	Maximum Flooded Area (km ²)			Mean Water Depth (m)			Mean Water Velocity (m/s)		
	NR	OS1	OS2	NR	OS1	OS2	NR	OS1	OS2
1978	555.59	550.94 -0.8 %	529.37 -4.7 %	2.41	2.27 -5.8 %	1.87 -22.4 %	0.47	0.45 -4.3 %	0.36 -23.4 %
1979	565.49	561.91 -0.6 %	531.01 -6.1 %	2.57	2.54 -1.2 %	1.88 -26.8 %	0.51	0.50 -2.0 %	0.36 -29.4 %
1989	530.98	528.31 -0.5 %	480.41 -9.5 %	1.86	1.84 -1.1 %	1.35 -27.4 %	0.36	0.35 -2.8 %	0.25 -30.6 %

670 **Table 3.** Hydraulic characteristic of most extreme flood events in the lower Tagus valley considering the outflows provided
 by the different dam configurations considered (*Simulation_Dam*). NR is referred to the natural regime (no dam), OS1 is
 referred to the operation strategy presented in equation (4), and OS2 is referred to the operation strategy focused on extreme
 events presented in equation (5). The percentage values represent the reduction obtained with respect to the situation under
 natural regime. The events occurred in 1972 and 1997 were not included in the hydraulic analysis because they can be
 675 avoided at Alcántara location (see Table 2).

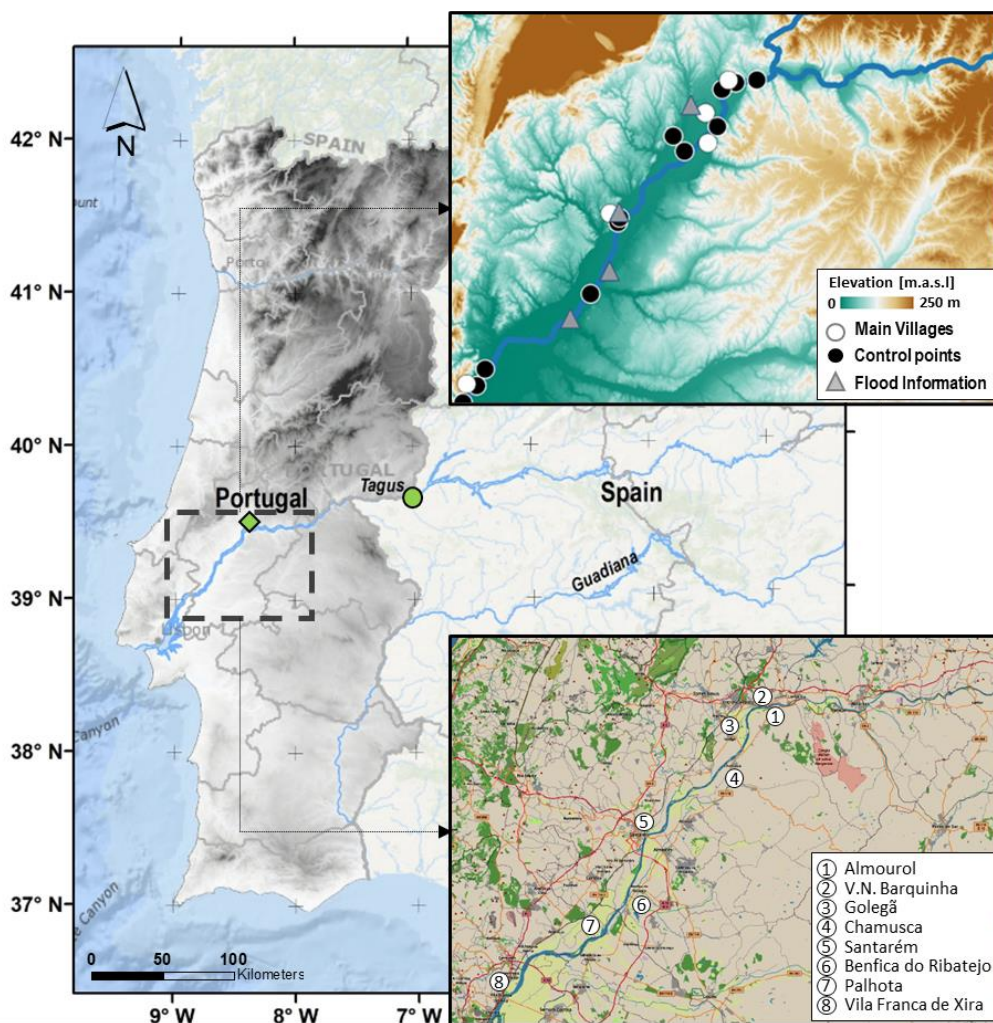
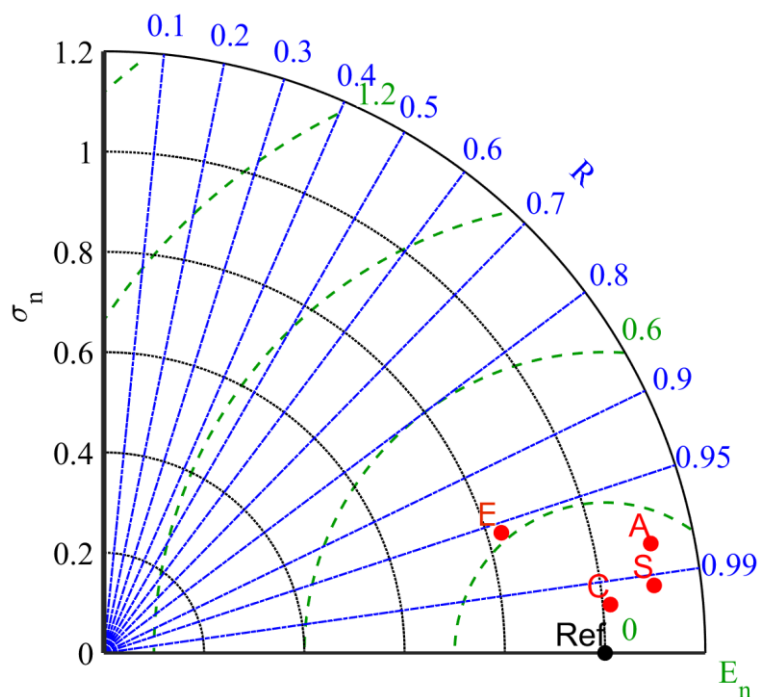


Figure 1. Area of study. Left panel indicates the location of the study area (dashed black rectangle) including the lower Tagus valley. Green diamond indicates the location of Almourol station and green circle indicates the location of Alcántara dam. The right panels represent the basin under scope. In the upper right panel, the black circles represent the control points where there is data on the water levels reached in the 1979 flood event. The grey triangles represent areas with relevant flood information (particular flooded areas, water depths...) for the 1979 event, from north to south: railroad of Golegã, Santa Iria statue at Santarem, football field at Benfca do Ribatejo, and Palhota town. The white circles indicate the location of the main villages affected by the flood: from north to south: V.N. da Barquinha, Golegã, Chamusca, Santarém and Vila Franca da Xira. In the lower right panel, the main locations of interest are represented. Bathymetry and topography basemaps were provided by ESRI©.



690 **Figure 2.** Taylor diagram of the water elevation obtained with Iber+ using the field data as reference. E, A, S and C indicate
the Iber+ data obtained using the ESRI, ASTER, SRTM and Copernicus Digital Elevation Models.

695

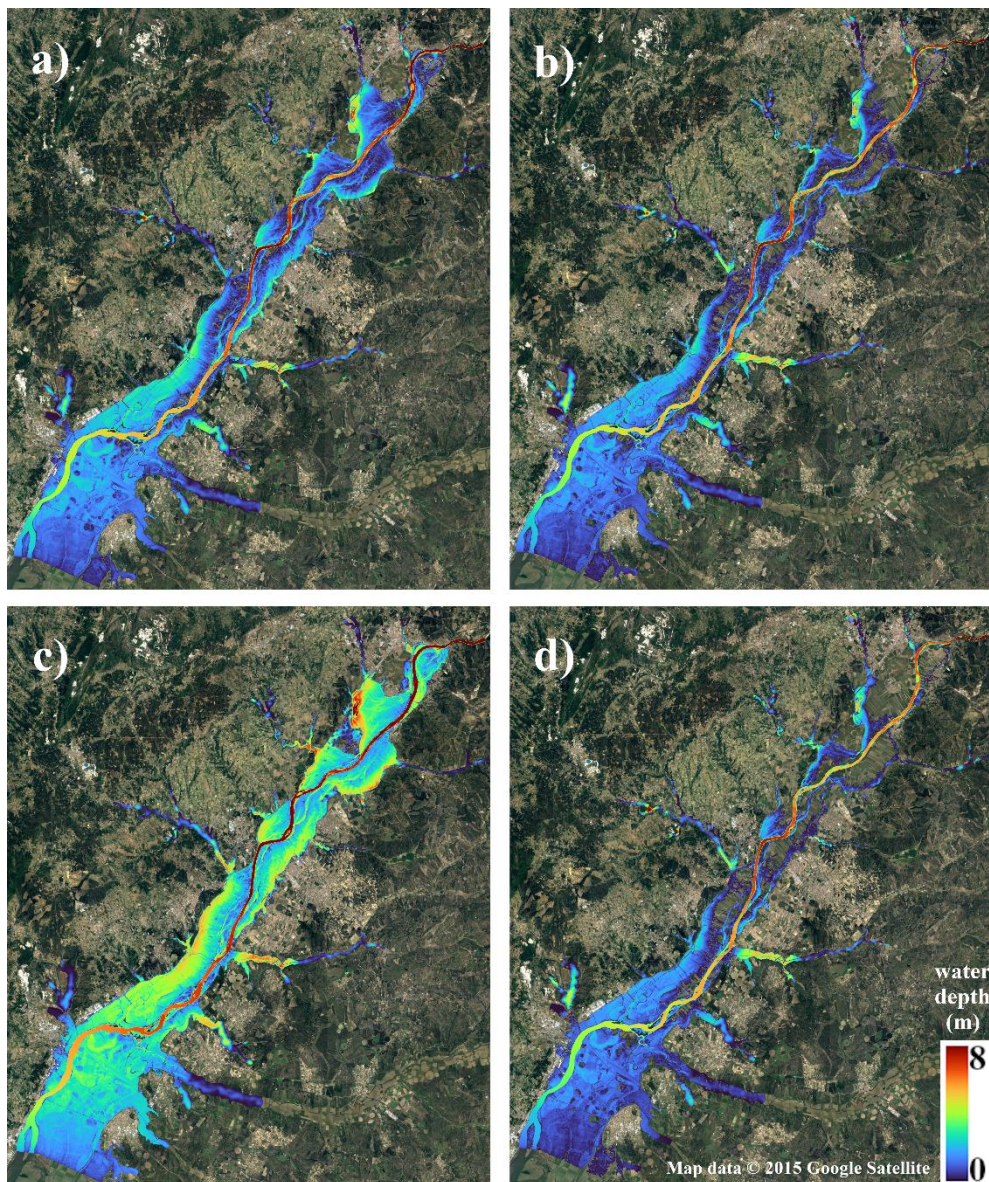


Figure 3. Reproduction of water depth (meters) for the flood event occurred in February, 1979 in lower Tagus valley, using
700 Iber+ hydraulic model. a), b), c) and d) represents the flood situation on 5, 8, 11 and 16 February under the
Simulation_Control_1979.



Figure 4. Maximum flood extension for event of February, 1979, in lower Tagus, obtained from the hydraulic simulation (Simulation_Control_1979). The white line represents the real extension of the flood reconstructed by the National Civil Engineering Laboratory (LNEC) and the Water Institute (INAG) from Portugal (www.snirh.pt).

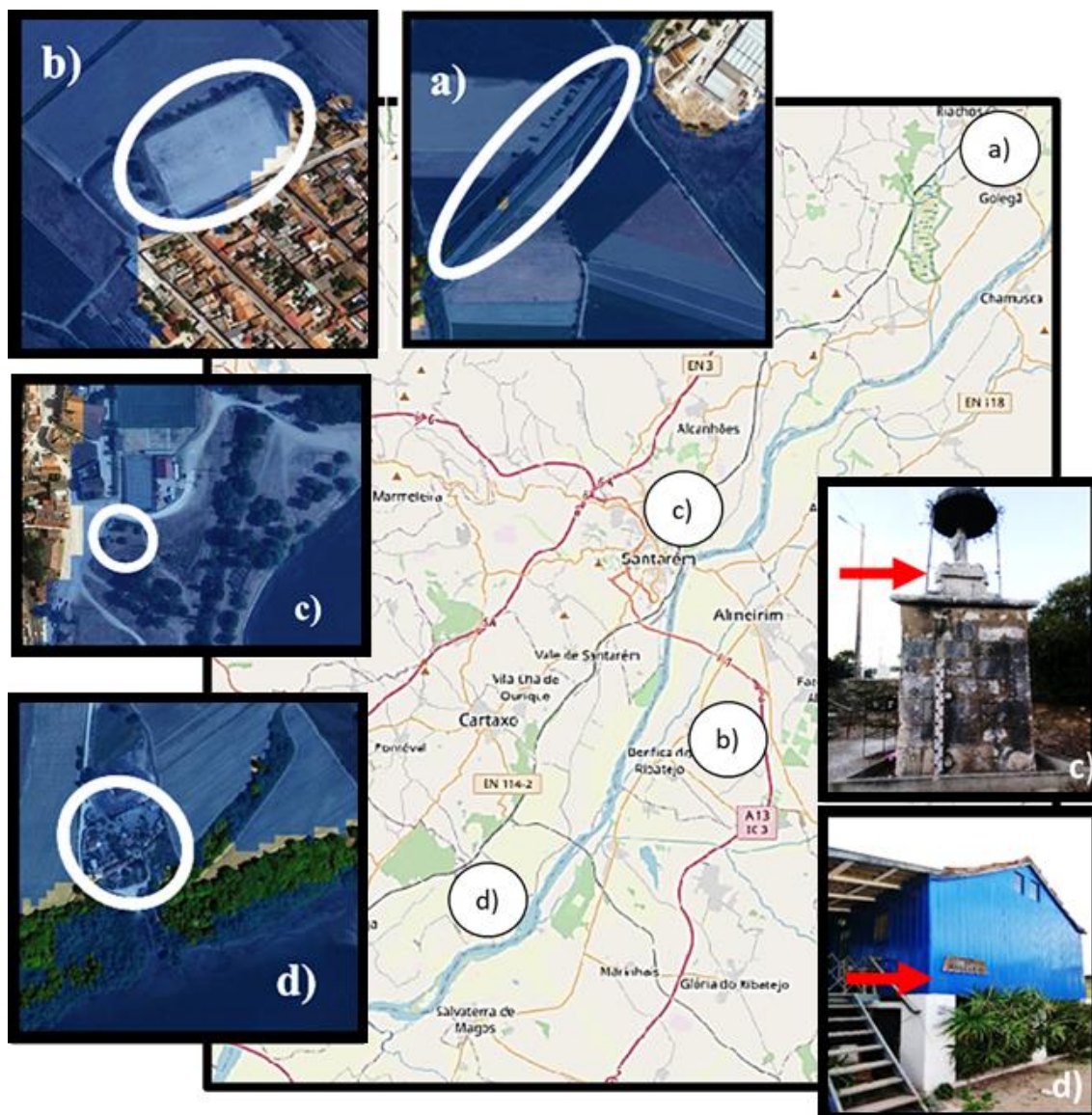
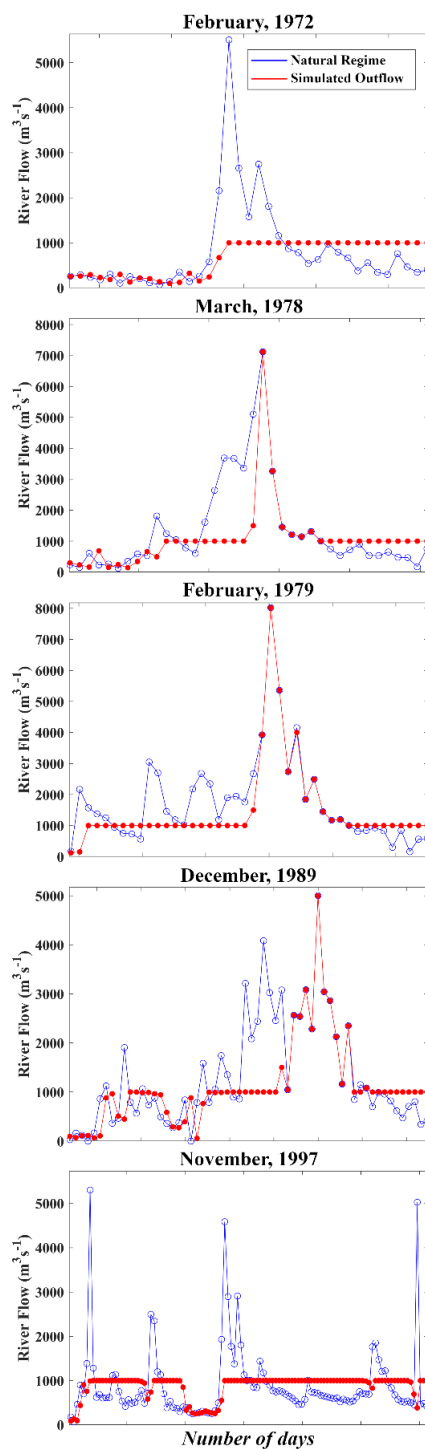
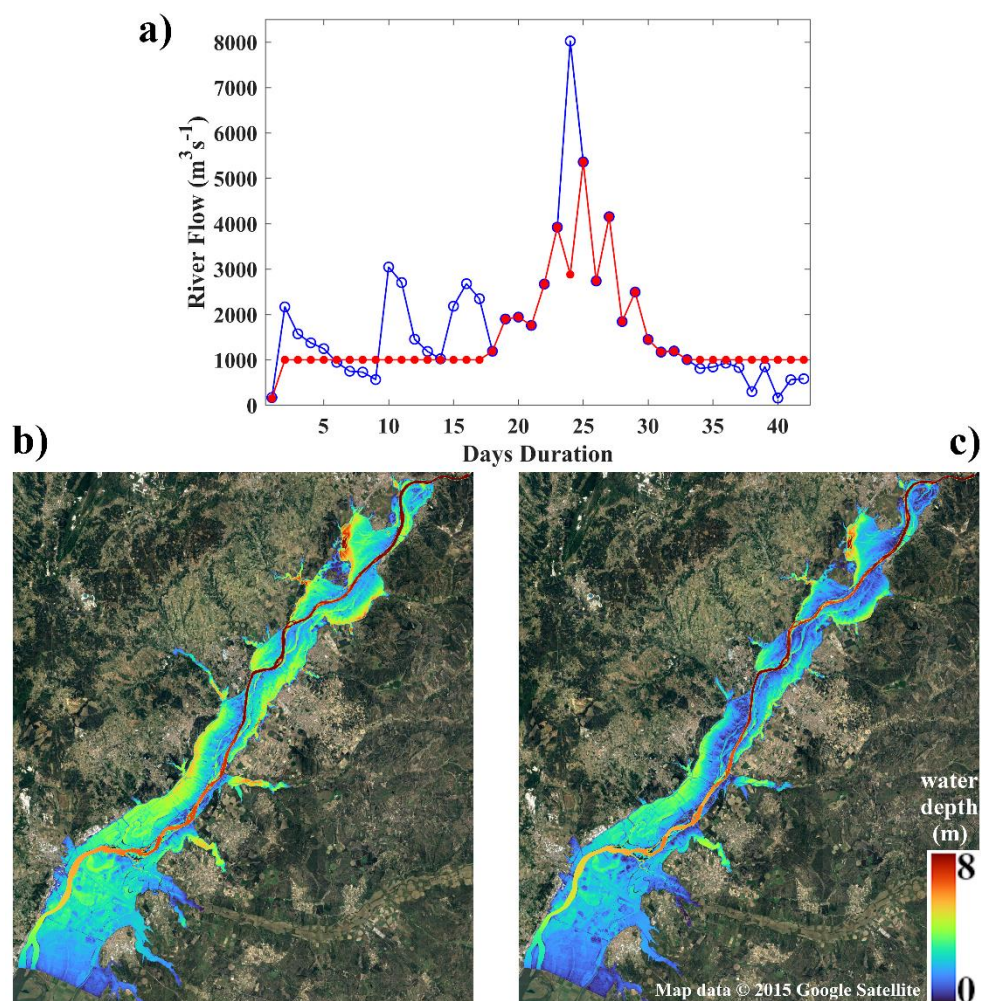


Figure 5. Detailed flooded area obtained with hydraulic simulation (Simulation_Control_1979) for: a) railroad of Golegã, b) football field at Benfica do Ribatejo, c) Santa Iria statue at Santarém, and d) Palhota town. The red arrow indicates the level reached by the water. The photographs and measurements in panels c) and d) were taken by the authors. Aerial maps in panels a), b), c) and d) from: Map data © 2015 Google Satellite.

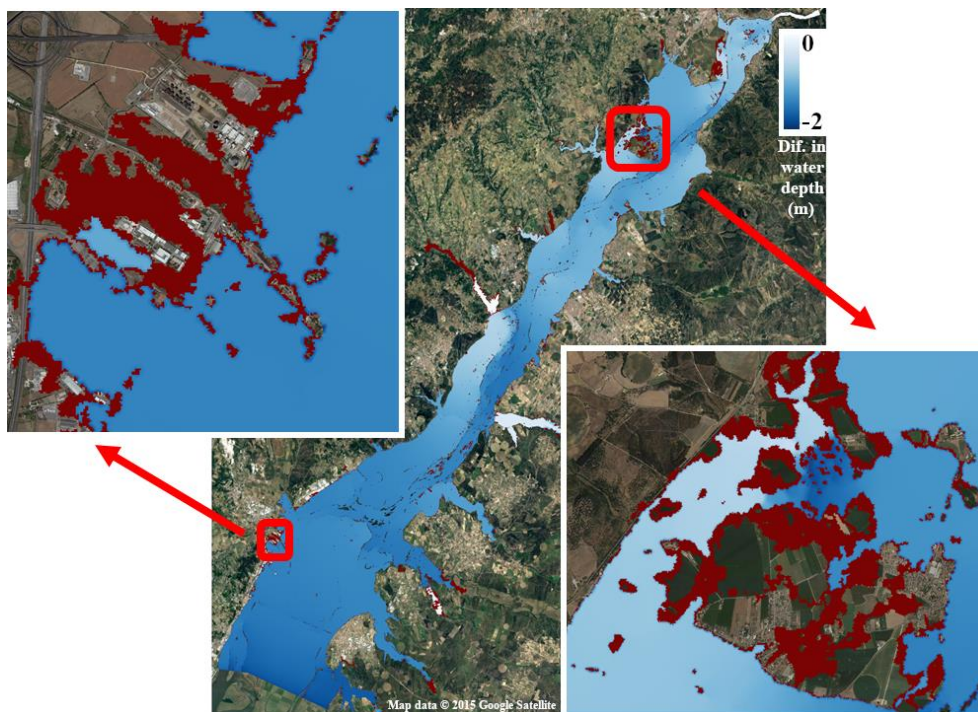


715

Figure 6. Natural regime (blue line) and simulated outflow resulting for the operation strategy OS1 of equation (4) (red line) for Alcántara dam in the most extreme cases. The date is referred to the occurrence of the highest peak flow.



720 **Figure 7.** (a) Natural regime at Alcántara (blue line) and simulated Alcántara dam outflow under the operation strategy OS2 (red line), considering the flooding of 1979. Lower panels show the maximum water depth (meters) obtained with Iber+ for the outflows corresponding to (b) natural regime, and (c) dam operation strategy OS2, applied to the 1979 flood event.



725 **Figure 8.** Difference in maximum water depth (meters) caused by the Alcántara outflows corresponding to natural regime
(NR) and operation strategy OS2 (OS2 – NR), applied to the 1979 flood event. Red colors represent locations reached by
water under the most extreme case (NR) and not flooded when OS2 is applied. The zoomed areas show the retraction in
flood extent that occurs when the most effective dam operation is applied. In particular, left zoomed area represents the
surroundings of Castanheira do Ribatejo town, whereas right zoomed area represents the zone delimited by the towns of
730 Mato de Miranda, Azinhaga and Pombalinho in the surroundings of Golegã location.